

# Intermittency in forced two-dimensional turbulence

W. Brent Daniel, Maarten A. Rutgers

*Department of Physics, The Ohio State University, 174 W. 18th Ave. Columbus, OH 43210  
(February 8, 2008)*

We find strong evidence for intermittency in forced two dimensional (2D) turbulence in a flowing soap film experiment. In the forward enstrophy cascade the structure function scaling exponents are nearly indistinguishable from 3D studies. Intermittency corrections are present in the inverse energy cascade as well, but weaker. Stretched exponential tails of the velocity difference probability distribution functions and shock like events at large velocity differences also resemble 3D studies. For decaying turbulence, where only the forward enstrophy cascade remains, all signs of intermittency disappear.

PACS numbers: 47.27.Gs, 68.15.+e

Energy dissipation in three dimensional (3D) turbulence is punctuated by intermittent bursts [1] and it has been conjectured that intense vortex filaments are responsible for these bursts [2]. Since vortex filaments cannot exist in two dimensions (2D) it is perhaps not surprising that recent experiments by Paret and Tabeling on the inverse energy and forward enstrophy cascades of 2D turbulence have found no signs of intermittency [3,4]. Simulations by Smith and Yakhot [5] for the inverse energy cascade agree with these experiments, but simulations by Babiano, Dubrulle, and Frick [6] do not. The latter simulations go beyond the experiments in that they explore not only the isolated inverse energy and forward enstrophy cascades but also simultaneous cascades. In each case Babiano *et al.* find intermittency only in the energy cascade, which is partly at odds with the experiments. Further work could resolve such discrepancies. In this letter we report on 2D turbulence experiments in flowing soap films which can probe an isolated enstrophy cascade, as done by Paret and Tabeling [4], or simultaneous cascades as simulated by Babiano *et al.* The presence of intermittency in 2D would call for fundamentally new ideas about the source of the phenomenon in 2D and perhaps even in 3D.

Kraichnan [7] proposed that there are two scaling regimes in the energy spectrum of isotropic homogeneous 2D turbulence. Energy conservation, accompanied by the assumption that the energy should depend only on the wavenumber  $k$  and the energy dissipation rate per unit mass  $\varepsilon$  leads to,  $E(k) = C\varepsilon^{2/3}k^{-5/3}$ . This follows the same dimensional arguments first applied to 3D turbulence by Kolmogorov [8]. In 2D there is a further constraint. The mean square vorticity, or enstrophy ( $\Omega = 1/2 |\nabla \times \mathbf{v}|^2$ ), must also be conserved. Through the same considerations as above, namely the dependence on  $k$  and the enstrophy dissipation rate per unit mass  $\eta$ , we find  $E(k) = C'\eta^{2/3}k^{-3}$ . This implies the existence of a second cascade, the enstrophy cascade. In order for the two cascades to be present simultaneously, Kraichnan proposed a forward enstrophy cascade and an inverse enstrophy cascade [7].

It is in these two inertial ranges that we look for the

presence of intermittency. A particularly useful tool is the velocity difference, or increment, between two points separated by a vector  $\mathbf{r}$ ,  $\delta\mathbf{v}(\mathbf{x}, \mathbf{r}) = \mathbf{v}(\mathbf{x}+\mathbf{r}) - \mathbf{v}(\mathbf{x})$ . In the present experiment we take both  $\mathbf{v}$  and  $\mathbf{r}$  along the direction of the mean flow. Using this quantity it becomes possible to probe the statistics of the flow as a function of length scale  $r$ . If the turbulent velocity field is self similar with respect to  $r$ , then the probability distribution functions  $P(\delta v(r))$  should scale with  $r$ , as was the case in the experiments of Paret and Tabeling [3,4]. Intermittent events break the self similarity of the flow field and subsequently lead to  $P(\delta v(r))$  which do not scale with  $r$ .

This deviation from self-similarity is also manifest in the moments of the velocity differences, collectively known as the structure functions,

$$S_p(r) = \langle \delta v^p(r) \rangle = \int_{-\infty}^{\infty} \delta v^p P(\delta v(r)) d(\delta v). \quad (1)$$

We also define a second function,  $G_p(r) = \langle |\delta v(r)|^p \rangle$ , which is often calculated for odd  $p$  when a scaling range in  $S_p(r)$  is narrow or absent. Though the theoretical implications of  $G_p(r)$ , with  $p$  odd, are not yet clear we include it for completeness. In any case, results derived from  $G_{\text{odd}}(r)$  follow exactly the same trend as those derived from  $S_{\text{even}}(r) \equiv G_{\text{even}}(r)$ .

The only exact result involving the structure functions is the 2D equivalent of Kolmogorov's four-fifths law, relating the third order structure function to the energy dissipation rate [3]. It gives,  $S_3(r) = \frac{3}{2}\varepsilon r$ . Though no analytic relation has been derived for structure functions of higher orders, self-similarity implies that the structure functions should scale like  $S_p(r) \propto r^{\zeta_p}$ , with  $\zeta_p = p/3$  in the energy cascade. Dimensional analysis also suggests that  $S_3(r) \propto r^3$  and  $\zeta_p = p$  in the enstrophy cascade [9]. However, because we will look at the scaling exponents using the extended self-similarity (ESS) [10] hypothesis in the analysis of the structure functions, the results expected in the absence of intermittency will be the same in the enstrophy cascade as those in the energy cascade.

The present experiment makes measurements on a flowing soap film suspended between two taut vertical

nylon wires using an apparatus similar to that of previous experiments [11]. Two combs, each 64 cm long, are placed in the film so that they form an inverted wedge 1.2 cm apart at the top and 8 cm apart at the bottom. The cylindrical teeth have an average spacing of 1.6 mm and a diameter of 0.22 mm. The geometry of the combs and the positions where data was collected are shown on the right of Fig. 1. This particular orientation of the combs was found to produce the most isotropic and homogeneous turbulence, with a nearly Gaussian velocity distribution and a turbulence intensity low enough to rely on Taylor's frozen turbulence assumption.

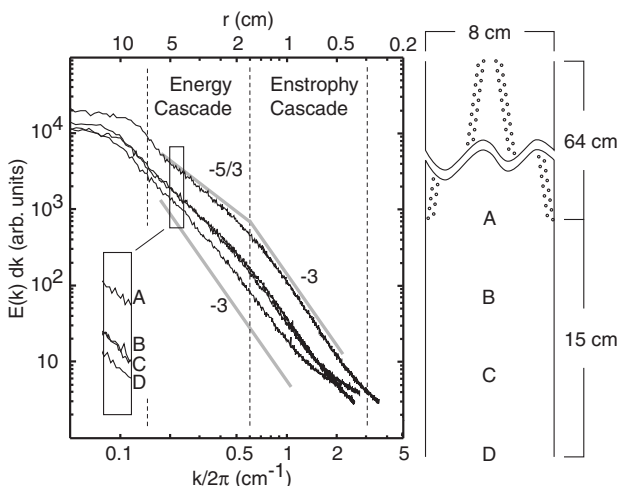


FIG. 1. Energy spectra at locations A though D as noted at right. The energy and enstrophy cascade ranges are with respect to curve A, the fully forced case. Theoretically predicted energy and enstrophy scaling exponents are provided for comparison with the data.

A laser velocimetry system (LDV) from TSI Inc. is used to make the velocity measurements. Data is taken for two hours in the center of the film at each of four vertical locations to obtain data sets of 33.6 million points each. Roughly 14 kilometers of film flows past the measurement location during the taking of each data set, with velocities being recorded every 0.4 mm on average (with a typical data rate of 5kHz). The mean velocity of the film at location (A) in Fig. 1 is  $\bar{v} = 214 \text{ cm/s}$  with a root mean square deviation  $\langle \Delta v^2 \rangle^{1/2} = 21 \text{ cm/s}$  (where  $\Delta v = v - \bar{v}$ ). The turbulence intensity is therefore  $I_t = 9.8\%$  at point A, less than half of values reported in other work on 3D turbulence [12,13]. At locations progressively farther below the combs we see a corresponding change in the magnitude of the turbulence intensity, decreasing to 8.0% at B, 6.8% at C, and 6.0% at D.

From the data sets, the  $P(\delta v(r))$  were calculated at various values of  $r$ , and from these, the functions  $G_p(r)$  were calculated by numerical integration akin to Eq. 1. It should be noted that there is an inherent limitation on the maximum order of the structure function that can be calculated in any physical experiment. As  $p$  is increased

the majority of the weight of the integrand comes increasingly from the tails of the PDFs, where the number of data points becomes quite small. We found that the majority of the weight of the numerical integration of  $G_p(r)$  was not contributed by the wings of the PDFs for  $p \leq 14$ .

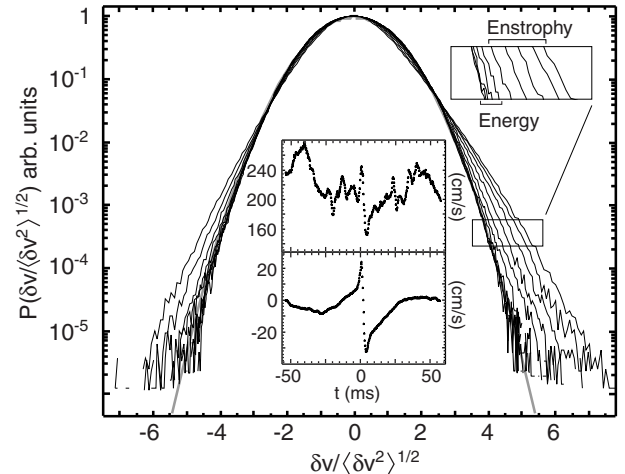


FIG. 2. Normalized velocity difference probability distributions for a range of separations through the energy and enstrophy cascades from data taken at location A. The thick gray line is a Gaussian reference curve. The upper inset shows one particularly steep velocity fluctuation event representative of the wings of the distributions. The lower inset is an average of all such events with  $|\delta v / \langle \delta v^2 \rangle^{1/2}| \geq 5.35$  at a separation of 0.5 cm (there were a total of 311).

Furthermore, as suggested by Anselmet *et al.* [13], the convergence of the structure functions with an increase in the size of the data set provides a check on the quality and quantity of the data. If each small subset of the data is statistically identical to all other subsets, we expect to arrive at the same value for the  $G_p(r)$  regardless of the size of the subset used in the calculation or which subset in particular is chosen. We find that for all separations  $r$ , the variation of  $G_6(r)$  is below 5% for data sets of  $5 \cdot 10^6$  points or greater. For  $G_{12}(r)$ ,  $25 \cdot 10^6$  points are needed to meet the same requirement. Given the above considerations we are confident of the measured structure functions up to order 12.

The energy spectrum in Fig. 1 shows simultaneous evidence of the two scaling regimes, with  $E(k) \propto k^{-5/3}$  in the inverse energy cascade (associated with driven turbulence) and  $E(k) \propto k^{-3}$  in the forward enstrophy cascade (associated with decaying turbulence). The location of the bend between the two scaling ranges gives an estimate of the effective injection length scale at each location. We estimate it to be  $k/2\pi = 1/\lambda = 0.63 \text{ cm}^{-1}$  or  $\lambda = 1.6 \text{ cm}$  at location A. Subsequent figures will refer to the energy and enstrophy cascades which are inferred from the spectrum at A. More details on the turbulent spectra and the nature of the injection scale were previously published by Rutgers [11].

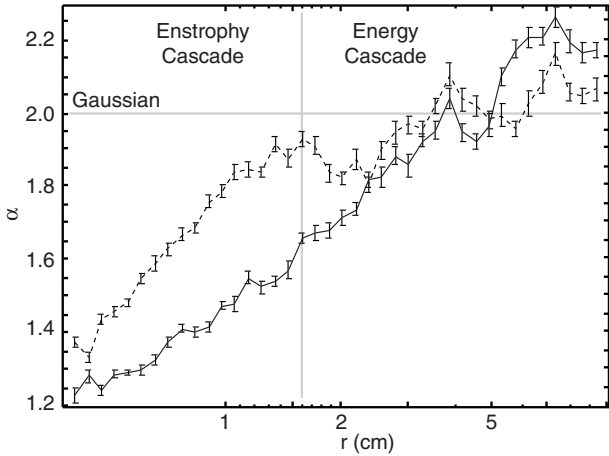


FIG. 3. The exponent  $\alpha$  of the best fit stretched exponential function  $P(\delta v) \propto \exp\{-|\delta v/\sigma|^\alpha\}$  (for data from location A). The solid line is the fit for  $\delta v/(\delta v^2)^{1/2} > 2$  (i.e. right wing); the dashed line corresponds to  $\delta v/(\delta v^2)^{1/2} < -2$  (left wing).

With the energy and enstrophy cascade inertial ranges defined, we inspect the data for signs of intermittency. Recent experiments on the separate energy and enstrophy cascades of a quasi 2D experimental system by Paret and Tabeling [3,4] found Gaussian velocity difference PDFs independent of the scale and concluded that there was a complete absence of intermittency. From the analysis of our forced turbulent data (measured at point A), we conclude quite the opposite. Figure 2 shows  $P(\delta v(r))$  for  $r$  covering both the forward enstrophy and inverse energy cascades. To accentuate relative shape changes the width of each distribution was rescaled by its second moment. The distributions with  $r$  in the energy cascade are close to Gaussian and differ substantially from distributions with  $r$  in the enstrophy cascade, which are decidedly more exponential in nature. This variation of the shape can be quantified by fitting the distributions to a stretched exponential function [12,14],  $P(\delta v) \propto \exp\{-|\delta v/\sigma|^\alpha\}$ . The dependence of the stretching exponent  $\alpha$  on  $r$  suggests a flow-field which is not self-similar and is an indication of intermittent turbulent flow. The positive and negative tails of the PDFs beyond  $2\sigma$  are then fit independently [12,14]. The trend toward a slower than Gaussian falloff at small length scales is shown in Fig. 3. The minimum  $\alpha$  for negative  $\delta v$  is greater than for positive  $\delta v$  reflecting the inherent asymmetry. Note that the sign of the asymmetry is in keeping with the exact theoretical result,  $S_3(r) = \frac{3}{2}\varepsilon r$ .

The events in the raw velocity data which populate the wings of the  $P(\delta v(r))$  can be singled out. A typical event is shown in the upper inset of Fig. 2. The lower inset shows an average of all such events for  $r = 0.5$  cm and  $|\delta v(r)/(\delta v(r)^2)^{1/2}| \geq 5.35$  (an arbitrary cutoff). Since the third moment of  $P(\delta v(r))$  is positive, the average has a corresponding characteristic sharp negative slope. Note that the insets in Fig. 2 have been plotted as

raw time traces from the measurement probe, as is customarily done in previous work. The application of the frozen turbulence assumption will lead to a shock with positive slope which gives a positive  $S_3(r)$  for our definition of  $\delta v(r)$ . The shock-like nature of these events bears a strong qualitative resemblance to intermittent events measured in 3D turbulence, but typically with a velocity increment of opposite sign [15,16], since  $S_3(r)$  is negative for 3D turbulence.

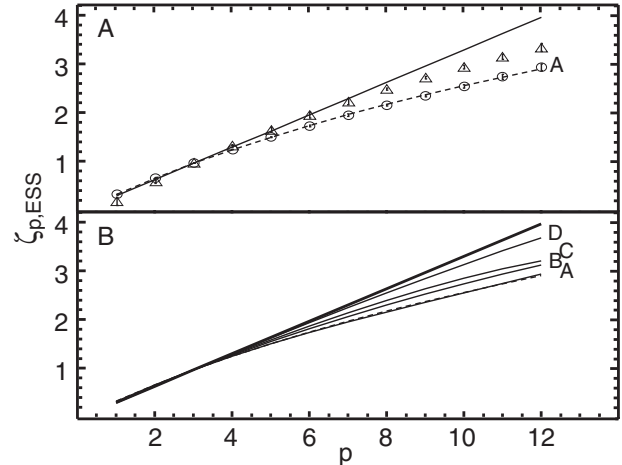


FIG. 4. **A.** ESS scaling exponents in the inverse energy ( $\triangle$ ) and forward enstrophy ( $\circ$ ) cascades at location (A) (see Fig. 1). The solid line is the K41 prediction, and the dashed line the log-Poisson. Error bars show the 95% confidence interval. **B.** Measurements of  $\zeta_{p,\text{ESS}}$  in the enstrophy range at points A,B,C, and D (see Fig. 1)

These intermittent events have a strong effect on the structure functions  $S_p(r)$ , which theoretically scale with  $r$ . Practically, it is extremely difficult to discern this scaling directly since one typically requires several decades of clearly discernible scaling in  $E(k)$ . Most experiments, ours included, do not have that luxury. The standard remedy follows a technique introduced by Benzi *et al.* [10] where  $S_p(r)$  is plotted against  $G_3(r)$ , leading to much cleaner power laws throughout the inertial range. This procedure is referred to as extended self-similarity and is used in most studies of intermittency in 2D and 3D turbulence. We will refer to the scaling exponents derived from this technique as  $\zeta_{p,\text{ESS}}$ . Figure 4A shows the  $\zeta_{p,\text{ESS}}$  as a function of the order  $p$ , for data collected at point A. The solid line is the prediction in the absence of intermittency, and the dashed curve the log-Poisson prediction [17] (which is a good fit to the canonical 3D intermittency measurements of Anselmet *et al.* [13]). Our scaling exponents from the enstrophy cascade of forced 2D turbulence ( $\circ$ ) are nearly indistinguishable from those for 3D measurements. Exponents from the energy cascade deviate as well from the self-similar prediction, but to a lesser degree ( $\triangle$ ).

At first sight our measurements appear to contradict those of Paret and Tabeling mentioned earlier [3,4].

There is, however, an important difference between our measurements and theirs. Paret and Tabeling's electroconvection cell is limited by its range of accessible length scales and is capable of producing only the inverse energy cascade or the forward enstrophy cascade independently. Computer simulations are often similar in scope when they employ hyperviscous terms to suppress the enstrophy range when the energy range is being studied [5]. The results shown in Fig. 4 are for a system with *both* cascades present simultaneously.

To verify the importance of two cascades versus one, we performed the analysis leading to Fig. 4A again for points progressively further downstream from the combs where the turbulence has decayed (points B, C, and D in Fig. 1). The results are summarized in Fig. 4B. At the largest distance below the comb (D) the spectrum indicates only an enstrophy cascade [11,18,19]. Accordingly the indications of intermittency disappear with  $\zeta_p, \text{ESS}$  tending toward  $p/3$ . Our results at this location thus agree with the electroconvection experiments [4] on the isolated enstrophy cascade. We were not able to produce the case of an isolated energy cascade in the flowing soap films and thus, cannot make a comparison to the corresponding electroconvection experiments [3] which also found no intermittency. Soap film and electroconvection experiments therefore agree for similar situations, but both disagree with parts of simulations by Babiano *et al.*, which claim intermittency for inverse energy cascades but never for forward enstrophy cascades, regardless of whether the cascades are isolated or simultaneous.

There is always a question of the viability of flowing soap films as effective 2D incompressible fluids. It is possible that our results are influenced by quantities specific to flowing soap films, such as air drag, film thickness variations, or compressibility effects. Though these effects are important and we will make them the subject of further study, the clear identification of the energy and enstrophy cascades in flowing films [11,20] justifies this experimental medium. To this can be added our current agreement with electroconvection experiments [3,4] that there is no significant intermittency in 2D turbulent flows with an isolated enstrophy cascade.

In conclusion, find evidence of intermittency in forced 2D turbulence when both the inverse energy and forward enstrophy cascades are present simultaneously. Signs of intermittency are strongest in the enstrophy cascade, and present to a lesser degree in the energy cascade. Evidence of intermittency is threefold. First we find a considerable dependence of the shape of the velocity difference PDFs on the scale  $r$ . As  $r$  is increased through the enstrophy and energy cascade ranges the tails of  $P(\delta v(r))$  can be fit by a stretched exponential with exponent  $\alpha$  varying from 1.23 toward Gaussian statistics. Secondly we can identify shock like changes in the velocity which contribute to the tails of  $P(\delta v(r))$ . Thirdly, there is a deviation of the ESS structure function scaling exponents from the K41 pre-

diction in both the energy and enstrophy cascades. The experimental values lie well-below the K41 prediction of  $\zeta_p = p/3$  in the energy cascade, and in the enstrophy cascade lie directly on top of the log-Poisson prediction [17]. The same system shows none of these signs of intermittency when the turbulence is left to decay, in which case there is only an isolated enstrophy cascade. This observation agrees with other experiments using an electroconvection technique [4]. The simultaneous presence of both inverse energy and forward enstrophy cascades appears necessary to observe intermittency in 2D turbulence.

## ACKNOWLEDGMENTS

We would like to thank C. Jayaprakash and F. Hayot for their stimulating discussions. The present work was supported by the Petroleum Research Foundation and The Ohio State University.

- 
- [1] G. Batchelor and A. Townsend, Proc. R. Soc. Lond. A **199**, 238 (1949).
  - [2] U. Frisch, *Turbulence: The Legacy of A. N. Kolmogorov* (Cambridge University Press, Cambridge, 1995).
  - [3] J. Paret and P. Tabeling, Phys. Fluids **10**, 3126 (1998).
  - [4] J. Paret, M. Jullien, and P. Tabeling, Phys. Rev. Lett. **83**, 3418 (1999).
  - [5] L. Smith and V. Yakhot, J. Fluid Mech. **274**, 115 (1994).
  - [6] A. Babiano, B. Dubrulle, and P. Frick, Phys. Rev. E **52**, 3719 (1995).
  - [7] R. Kraichnan, Phys. Fluids **10**, 1417 (1967).
  - [8] A. Kolmogorov, Dokl. Akad. Nauk SSSR **30**, 299 (1941).
  - [9] R. Benzi, G. Paladin, S. Patarnello, P. Santangelo, and A. Vulpiani, J. Phys. A **19**, 3771 (1986).
  - [10] R. Benzi, S. Ciliberto, R. Tripiccione, C. Baudet, F. Massaioli, and S. Succi, Phys. Rev. E **48**, R29 (1993).
  - [11] M. Rutgers, Phys. Rev. Lett. **81**, 2244 (1998).
  - [12] P. Tabeling, G. Zocchi, F. Belin, J. Maurer, and H. Willaime, Phys. Rev. E **53**, 1613 (1996).
  - [13] A. Anselmet, Y. Gagne, E. J. Hopfinger, and R. A. Antonia, J. Fluid Mech. **140**, 63 (1984).
  - [14] K. R. Kailasnath, K. R. Sreenivasan, and G. Stolovitzky, Phys. Rev. Lett. **68**, 2766 (1992).
  - [15] F. Belin, J. Maurer, P. Tabeling, and H. Willaime, Physica Scripta **T67**, 101 (1996).
  - [16] H. Willaime, F. Belin, and P. Tabeling, European Journal of Mechanics B **17**, 489 (1998).
  - [17] Z. She and E. Leveque, Phys. Rev. Lett. **72**, 336 (1994).
  - [18] G. Batchelor, Phys. Fluids Suppl. II **12**, 233 (1969).
  - [19] J. Chasnov, Phys. Fluids **9**, 171 (1997).
  - [20] B. Martin and X. Wu, Phys. Rev. Lett. **80**, 1892 (1998).